Journal of Computer-Aided Molecular Design, 9 (1995) 131–138
ESCOM

J-CAMD 286

LFER and CoMFA studies on optical resolution of α-alkyl α-aryloxy acetic acid methyl esters on DACH-DNB chiral stationary phase

Angelo Carotti[a,*], Cosimo Altomare[a], Saverio Cellamare[a], AnnaMaria Monforte[b], Giancarlo Bettoni[a], Fulvio Loiodice[a], Nicola Tangari[a] and Vincenzo Tortorella[a]

[a]*Dipartimento Farmacochimico, Università degli Studi di Bari, via E. Orabona 4, I-70126 Bari, Italy*
[b]*Dipartimento Farmacochimico, Università di Messina, I-90168 Messina, Italy*

Received 26 July 1994
Accepted 21 November 1994

Keywords: Chiral chromatography; Enantioseparation; CoMFA; 3D QSAR

Summary

The HPLC resolution of a series of racemic α-substituted α-aryloxy acetic acid methyl esters **I** on a π-acid chiral stationary phase containing *N,N'*-(3,5-dinitrobenzoyl)-*trans*-1,2-diaminocyclohexane as chiral selector was modelled by linear free energy-related (LFER) equations and comparative molecular field analysis (CoMFA). Our results indicate that the retention process mainly depends on solute lipophilicity and steric properties, whereas enantioselectivity is primarily influenced by electrostatic and steric interactions. CoMFA provided additional information with respect to the LFER study, allowed the mixing of different subsets of **I** and led to a quantitative 3D model of steric and electrostatic factors responsible for chiral recognition.

Introduction

In recent years, considerable dispute has arisen about the advantage of administering therapeutic agents as single isomers [1–4]. Optical antipodes of many drugs, in fact, have been proven to display different degrees of activity and toxicity [5,6].

Many efforts have therefore been addressed to the discovery of new and economical enantioselective syntheses [7] and to the development of techniques to achieve enantioseparation [8–10]. Among them, high-performance liquid chromatography on chiral stationary phases (CSPs) has been found to be the most useful and versatile technique for the resolution of enantiomeric mixtures on both analytical and preparative scale [11].

Many mechanistic studies have been carried out on chiral recognition [12] but, despite some recent significant advances [13], a satisfactory knowledge of the molecular mechanism(s) underlying chiral separation on CSPs has not yet been achieved.

Very recently [14], a new research strategy based on the coordinated use of quantitative structure–property relationships and molecular modelling techniques, namely docking and Comparative Molecular Field Analysis (CoMFA), has been successfully applied to the study of a series of alkyl–aryl sulfoxides resolved on DACH-DNB, a π-acid CSP containing *N,N'*-(3,5-dinitrobenzoyl)-*trans*-1,2-diamino cyclohexane as chiral selector [15,16].

In this paper we report on the application of the same approach to the study of the enantioseparation of a suitably designed series of α-substituted α-aryloxy acetic acid methyl esters **I**.

The resolution of racemic mixtures of esters **I** has relevance from a biological viewpoint, since for the pure optical isomers of the corresponding acids a favourable dissociation of the pharmacological properties has been observed [17]. In fact, *R*-isomers showed antilipidemic effects comparable to those of *S*-isomers, but higher anti-aggregatory activity and lower myotonic and hepatocarcinogenic effects [18]. Moreover, the two antipodes showed opposite effects on chloride ion conductance and excitation–contraction coupling of skeletal muscle [19].

The present study was aimed at detection of the main physicochemical interactions responsible for retention and enantioseparation of **I** on DACH-DNB CSP. A comparison with the results previously obtained with substituted

*To whom correspondence should be addressed.

sulfoxides **II** should yield further information on the physicochemical machinery used by DACH-DNB to perform chiral separations, and this in turn could contribute new ideas to the design of new improved CSPs.

Experimental

Chemicals and solvents

The preparation of analytical samples of methyl esters **I** was achieved by reacting the corresponding acids with an excess of diazomethane. The purity of each analyzed compound was routinely checked by TLC and RP-HPLC before chromatographic analysis on DACH-DNB CSP. HPLC-grade *n*-hexane and methylene chloride were degassed with helium before use.

Apparatus and chromatographic procedure

Analytical liquid chromatography was performed using a Waters 600 solvent delivery system (Waters, Milford, MA) equipped with a U6K injector and a 490 programmable multiwavelength detector. A modified JASCO J-500A spectropolarimeter (JASCO Europe, Cremella), equipped with a flow cell, was used for circular dichroism spectroscopy. All chromatographic measurements were carried out at a constant temperature of 25±1 °C on a DACH-DNB with 1*R*,2*R* absolute configuration [15] using methylene chloride–*n*-hexane (15:85) as the mobile phase. Compounds with absolute *R* configuration were eluted first on the *R,R* DACH-DNB CSP. The elution order was confirmed by monitoring the Cotton effect at 235–260 nm, where a negative sign was indicative of the *S* absolute configuration. Chiroptical data for the levo-α-4-chlorophenoxy-phenylacetic acid methyl ester **17**, complicated due to the presence of three different chromophoric systems, suggested an *S* configuration for the first eluted enantiomer; this inversion of the elution order has been explained [20] by the competition of phenyl and 4-chlorophenoxy groups for the π-acid sites of CSP. The absolute configuration of compound **17**, recently established by chemical correlation (V. Tortorella, unpublished results), proved that the levo isomer has *R* configuration.

Theoretical descriptors and computational methods

LCAO-MO theoretical indices of the functional groups (or atoms) possibly involved in the chiral recognition process were computed by the AM1 semiempirical quantum-mechanical method within the AMPAC suite of programs (QCPE Program 506). In particular, reactivity indices like electrophilic superdelocalizabilities as well as atomic net charges were calculated for selected atoms.

Correlation analysis

A cross-validated regression analysis was performed within the QSAR module of the SYBYL molecular

TABLE 1
DIRECT CHROMATOGRAPHIC RESOLUTION DATA AND EMPIRICAL AND THEORETICAL DESCRIPTORS USED IN THE QSERR STUDY OF METHYL ESTERS **I**[a]

Compound	X	R	R'	Log k'_R	Log k'_S	Log α	Log P	π_x	σ^-_x	$qC_{1'}$	S^H_{Ph}	v_R
1	H	CH_3	H	0.157	0.291	0.134	1.961	0.00	0.00	0.036	7.71	0.52
2	CH_3	CH_3	H	0.140	0.324	0.184	2.610	0.56	–0.17	0.028	7.62	0.52
3	F	CH_3	H	0.113	0.217	0.104	2.244	0.14	0.06	0.020	7.21	0.52
4	Cl	CH_3	H	0.111	0.255	0.144	2.814	0.71	0.23	0.036	6.92	0.52
5	Br	CH_3	H	0.149	0.303	0.154	2.964	0.86	0.23	0.050	6.50	0.52
6	OCH_3	CH_3	H	0.513	0.688	0.175	2.050	–0.02	–0.27	–0.002	7.60	0.52
7	$N(CH_3)_2$	CH_3	H	0.841	1.069	0.228	2.260	0.18	–0.83	–0.027	5.61	0.52
8	$COCH_3$	CH_3	H	1.259	1.309	0.050	1.701	–0.55	0.84	0.065	7.06	0.52
9	CN	CH_3	H	1.208	1.242	0.034	1.719	–0.57	0.88	0.067	6.81	0.52
10	NO_2	CH_3	H	0.979	1.008	0.029	2.004	–0.28	1.24	0.083	6.43	0.52
11	Cl	H	H	0.480	0.480	–	2.505	0.71	0.23	0.033	6.12	0.00
12	Cl	Et	H	0.048	0.206	0.158	3.343	0.71	0.23	0.037	6.92	0.56
13	Cl	*n*-Prop	H	0.014	0.193	0.179	3.872	0.71	0.23	0.037	6.90	0.68
14	Cl	*i*-Prop	H	–0.025	0.103	0.128	3.742	0.71	0.23	0.037	6.90	0.76
15	Cl	*n*-Hex	H	–0.038	0.165	0.203	5.459	0.71	0.23	0.046	6.91	0.68
16	Cl	CH_2Ph	H	0.184	0.320	0.136	4.382	0.71	0.23	0.036	6.67	0.70
17	Cl	Ph	H	0.281	0.369	0.088	4.064	0.71	0.23	0.035	6.81	0.57
18	Cl	Et	CH_3	–0.062	–0.062	0.000	3.652	0.71	0.23	0.045	6.98	1.08[b]
19	Cl	*n*-Prop	CH_3	0.112	0.112	0.000	4.181	0.71	0.23	0.046	6.97	1.13[b]

[a] k'_R, k'_S are capacity factors of the first and second eluted enantiomer, respectively; α is the enantioseparation factor; S^H_{Ph} represents the sum of the electrophilic superdelocalizabilities (kcal mol^{-1}, scaled by 100) calculated for the aromatic aryloxy carbons; $qC_{1'}$ is the total net charge on the aromatic carbon atom linked to the aryloxy oxygen; σ^- is the Hammett through-resonance electronic substituent constant; π is the Hansch hydrophobic constant from the benzene reference system; v is the Charton steric parameter. The subscripts X and R mean that the parameter values are referred to X and R substituents, respectively. For the structure of benzofuran methyl ester **20**, see Scheme 1.

[b] Estimated values for the R + R' alkyl substituents.

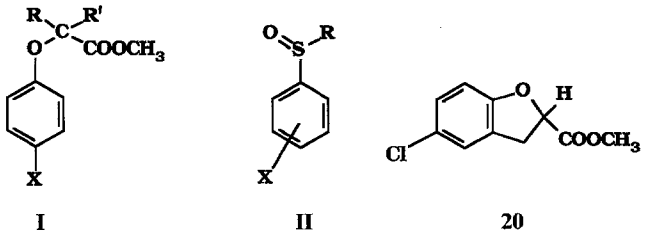

I II 20

Scheme 1. Structures of compound classes **I** and **II** and benzofuran methyl ester **20**.

modelling package (Tripos Associates, St. Louis, MO). The cross-validated squared correlation coefficient q^2 is defined as: $q^2 = SD - PRESS/SD$ where SD is the sum of squares of deviations of the observed values from their mean and PRESS is the prediction error sum of squares. q^2 gives an estimation of the predictive ability of the model.

Molecular modelling and CoMFA [21]

Molecular models of esters **I** were built using bond and angle standard geometries from SYBYL (v. 5.41) and were fully optimized by AM1 based on a preliminary conformational analysis carried out on parent compound **4**. To keep the computation time within reasonable limits, we explored the conformational space generated by changing the torsion angle defined by C_{ar}-O-C-C(O). A uniform scan was rigidly performed in steps of 15° for this torsion angle, with fixed values for all bond lengths and angles. To take into account variations in the dihedral angle that determines the rotation of the $COOCH_3$ group, the angle (O=)C-C-C-C was optimized at each step. The molecular models of the other esters **I** were built starting from the structure of the minimum energy conformer of parent compound **4** (extended conformations were assumed for aliphatic groups higher than methyl) and were fully optimized by AM1. These optimized structures were used for the calculation of theoretical descriptors.

All calculations and molecular manipulations were carried out on an Evans and Sutherland PS390 graphics device, connected to a Digital VAX station 3100.

Default settings were used throughout the CoMFA study. The electrostatic term was calculated for each grid point where the steric energy was higher than the steric cutoff (30 kcal mol^{-1}), i.e., the option 'drop electrostatic' was set to NO.

All esters in Table 1 were superposed on a low-energy conformer of the rigid, best resolved benzofuran methyl ester **20** (Scheme 1), selected as template, using the multifit procedure of SYBYL, and the AM1 charges were calculated. The resulting alignment is depicted in Fig. 1.

The steric and electrostatic potentials were calculated at each lattice point by using an sp^3 carbon probe carrying a +1 atomic charge. The lattice grid size in CoMFA had a resolution of 2.0 Å and the region dimensions were defined with the automatic mode 'molecular volume'.

CoMFA was performed in two sequential steps. In the first step, the optimal number of components was determined by using 10 components and a number of cross-validated groups equal to the number of analyzed compounds. In the second run, the analysis was repeated without cross-validation by using the optimal number of components determined in the first step. The results from the second analysis were used to draw the coefficient contour maps shown in Figs. 2 and 3.

Results and Discussion

The well-recognized influence of the absolute configuration of α-substituted α-aryloxy acetic acid alkyl esters (AAAE) on their numerous biological activities has stimulated several studies on their preparation through asymmetric syntheses [22] and on their enantioseparation on different CSPs. Very recently, investigations seeking the key molecular features responsible for the enantioseparation of AAAE on Chiracel OD [23] and on DACH-DNB [24] have been reported. In the latter case, due to the limited size of the data set analyzed, only the electronic effect on the enantioselectivity has been quantitatively examined.

For the present study, the series of α-substituted α-aryloxy acetic acid methyl esters in Table 1 was designed by selecting the X and R substituents so as to sample more adequately their electronic, lipophilic and steric properties. In particular, the X substituents were chosen to fully explore the electronic interactions with the CSP while R substituents were varied, keeping constant the X substituent (chlorine) so as to study the influence of lipophilicity and bulkyness of R on the retention and enantioseparation processes.

Our design strategy was based on the most accepted

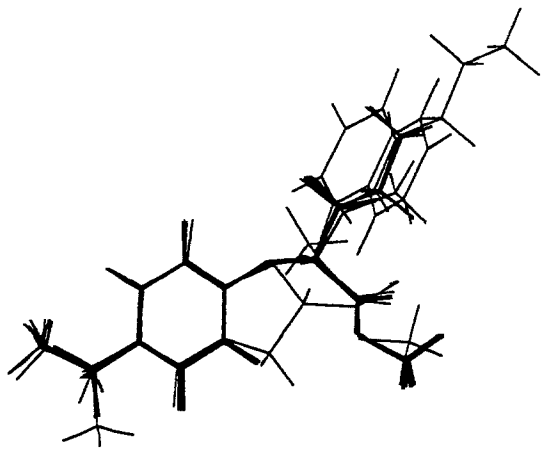

Fig. 1. Alignment of methyl esters **I** and **20** resulting from a multifit procedure and used in CoMFA.

knowledge regarding the mechanism of chiral recognition on Pirkle-type CSP [25] and on our recent findings on the resolution of sulfoxides **II** on DACH-DNB, according to which the main physicochemical forces governing chiral discrimination on Pirkle-type CSP are π–π stacking, dipole–dipole interactions, hydrogen bonding and steric repulsion.

To express the electronic properties of **I**, besides the classical σ^- Hammett through-resonance substituent constant [26], several theoretical electronic descriptors were computed by AM1 [27] and are reported in Table 1. As a measure of the π-basic character of esters **I**, the sum of the electrophilic superdelocalizability [28] of all the aromatic carbon atoms of the aryloxy ring, S^H_{Ph}, has been considered. $qC_{1'}$, the net charge of the aromatic carbon linked to the oxygen was also computed as a further indicator of the electronic properties of the X substituents. Moreover, following a recent proposal [29], the HB ability of the aryloxy oxygen was expressed by two theoretical descriptors (not reported): the electrophilic superdelocalizability S_o, taken as descriptor of the covalent component of HB, and the formal atomic net charge qO, accounting for the electrostatic component of HB. The bulkyness of the R groups was modelled by the Charton steric parameter ν [26]. Other parameters (not reported), i.e., the directional STERIMOL parameters L, B1, B5 [30], MR [26] and the 'excess of molar refractivity' ΔMR [31] were considered in the regression analysis. The lipophilicity was expressed by the estimated octanol–water partition coefficient (log P) [32].

In Table 1 the chromatographic resolution data from the racemic mixtures of **I** resolved on DACH-DNB are shown, together with some parameters and theoretical descriptors. The achiral derivative **11** was analyzed as reference compound to assess the influence of the R substituents on the retention process.

To transform qualitative observations into linear free energy-related (LFER) equations, a regression analysis with cross-validation was undertaken. Before analyzing and interpreting the retention and the discrimination processes it is important to realize that the CSP surface is not molecularly homogeneous, consisting not only of the chiral selector but also of unreacted free silanol and glycidoxypropylsilane moieties. All interactions with these different components should contribute to the retention (capacity factors k'), whereas only stereoselective interactions with the chiral selector should affect the enantioseparation (α).

As far as the retention is concerned, at first sight the capacity factors k' in the congeneric subset consisting of compounds **1**–**10** (set I) seem to be inversely related to the lipophilic character of the X para substituents, whereas the steric hindrance of R substituents appears to be mainly responsible for the k' variation along the other subset (compounds **11**–**19**; set II). By correlating the capacity factors of the most retained enantiomers (log k'_S) with steric, electronic and lipophilic parameters, for set I the best 'one-parameter' equations were (compound **1** omitted):

$$\log k'_S = -0.73\ (\pm 0.40)\ \pi_X + 0.80\ (\pm 0.20) \qquad (1)$$
$$n = 9;\ q^2 = 0.633;\ r^2 = 0.728;\ s = 0.251$$

and for set II:

$$\log k'_S = -0.41\ (\pm 0.18)\ \nu_R + 0.48\ (\pm 0.13) \qquad (2)$$
$$n = 10;\ q^2 = 0.620;\ r^2 = 0.852;\ s = 0.074$$

n, s, r^2 and q^2 are the number of data points, the standard deviation, the squared correlation coefficient and the cross-validated squared correlation coefficient, respectively; 95% confidence limits are reported in parentheses.

Adding other independent variables or combining the two sets resulted at best in marginal improvements of the statistics, indicating that the balance of intermolecular forces responsible for retention differs between the two sets of analytes examined. Equations 1 and 2 show that the retention is linked to lipophilic variation of X in set I and to steric properties of R in set II. According to our previous results, obtained for sulfoxides **II**, Eq. 1 could be interpreted taking into account the meaning of lipophilicity constant π_X. The partition coefficient-derived constant π_X is in fact a composite parameter which can be factorized into two terms, one representing bulk (or steric) properties (i.e., hydrophobicity), and the other related to electrostatic and polar properties [33]. The DACH-DNB CSP is a normal chromatographic phase, in which the selector is covalently bound to the silica matrix and hydrophobicity seems unlikely to contribute significantly to chiral recognition. Since it is well known that a silica gel surface is covered with layers of hydrogen-bonded water [34], the negative contribution of π_X may reflect the influence on the retention processes of the solute distribution between the polar silica gel surface and the apolar mobile phase [35]. Compounds **16** and **17** appeared to deviate from Eq. 2. Their 'higher than expected' log k'_S may indicate that other factors, most likely π–π interactions of both aromatic rings with the CSP, should be responsible for the enhancement of retention, as already observed [14]. The absence in the regression equations of a specific electronic term assessing the π-basic character of AAAE and/or the HB ability was quite surprising, since, as shown by us in the study of chiral recognition of sulfoxides **II**, this type of interactions affected retention on DACH-DNB. This difference between the LFER equations modelling the retention of compounds **I** and **II** apparently depends on the different electronic properties of sulfoxide and aryloxy oxygens.

As for enantioselection (see Eqs. 3–5 in Table 2), the variation of the separation factor (α) appears to be due

essentially to the electronic properties of X (Eq. 3) and the steric properties of R (Eq. 4). Equation 3, in full agreement with the analysis made by Tambuté [24], reveals that the highest enantioselectivity is presented by AAAE bearing strong electron-donor X substituents. Substitution of σ^- in Eq. 3 by $qC_{1'}$ resulted in an equation with a poorer fit ($r^2 = 0.755$). These findings are consistent with a mechanism involving π–π interaction between the aryloxy ring and the 3,5-dinitrobenzoyl moiety of DACH-DNB as a driving force for chiral discrimination. Equation 4 indicates that the enantioseparation is primarily driven by steric properties of R groups. The replacement of v with lipophilicity- or polarizability-related parameters resulted in less significant equations, confirming the bulkyness of R substituents as the main factor responsible for chiral recognition. The poor quality of Eq. 4 could be due to the non-homogeneity of set II (six monoalkyl, two dialkyl and two aryl R-substituted congeners). In fact, limiting the analysis to the more homogeneous alkyl sets, a significant improvement of the statistics was observed ($q^2 = 0.642$, $r^2 = 0.801$, $s = 0.040$). The duality of the results (Eqs. 3 and 4) and the non-overlapping of the parameter space explored by the two subsets render their mixing meaningless and statistically poor (Eq. 5).

Despite the helpful indications on the binding mode of **I** to DACH-DNB obtained from the analysis of Eqs. 1–5, further investigations were necessary to better assess structural factors involved in the chiral recognition and possibly to derive a model describing the enantioselection of the whole set of compounds. Therefore, a three-dimensional QSERR (Quantitative Structure–Enantioselective Retention Relationship) analysis was undertaken using the CoMFA approach [36].

Since its introduction in 1988, CoMFA has rapidly become a helpful tool to study 3D quantitative structure–property (activity) relationships, not only in medicinal chemistry but also in physical-organic chemistry. Very recently we reported encouraging results obtained applying CoMFA to study the interaction mechanism underlying the resolution of a variety of chiral sulfoxides on DACH-DNB CSP [14]. CoMFA methodology has been helpful to unravel the complexity of attractive and repulsive interactions occurring in chromatographic chiral recognition processes and to predict some enantioseparation factors.

Compound **20** was chosen as the reference molecule for superposition, because it was the best resolved on DACH-DNB and the most rigid in the set examined (see Fig. 1). In the derivation of a CoMFA model describing the enantioseparation, the achiral compound **11** was of course omitted. Compound **20**, carrying unique structural features, was first eliminated from the analysis as well. The initial regression equation was derived by using the cross-validation procedure [37]. A final CoMFA model, rationalizing about 97% of the variance in the log α values, and having predictive value (cross-validated $r^2 = 0.629$), was derived by using only the first four components. The electrostatic potential appears to be the major contributor to log α (58.3%). CoMFA results obtained on sets I and II and on the whole set are reported in Table 2.

Less predictive CoMFA models were obtained for the capacity factors of the single enantiomers ($q^2 = 0.407$ (3) and 0.457 (3) for log k'_R and log k'_S, respectively).

Looking at the statistical parameters in Table 2 we note that, while the results of LFER analysis and CoMFA are quite comparable for the individual subsets, the CoMFA model of enantioselection for the full data set (Eq. 8) is better than the LFER equation (Eq. 5) both in predictability and in fitting. Apparently, CoMFA parameters, accounting for the electrostatic and steric features of both X and R substituents, give a better description of the forces involved in chiral recognition than do Hammett constants (only for X) and Charton parameters (only for R).

The steric and electrostatic coefficient contour maps (Figs. 2 and 3, respectively) show regions where variations

TABLE 2
LFER AND CoMFA MODELS OF THE ENANTIOSEPARATION

Equation no.	Models	n	$q^{2\,a}$	r^2	s
LFER					
3	$\log \alpha = -0.10(\pm 0.03)\ \sigma^- + 0.15(\pm 0.02)$	10[b]	0.867	0.904	0.022
4	$\log \alpha = -0.27(\pm 0.17)\ v_R + 0.31(\pm 0.13)$	9[c]	0.479	0.651	0.046
5	$\log \alpha = -0.10(\pm 0.05)\ \sigma^- - 0.18(\pm 0.11)\ v_R + 0.25(\pm 0.08)$	18[d]	0.568	0.681	0.042
CoMFA					
6	log α vs. electrostatic fields	10[b]	0.688 (2)	0.903	0.024
7	log α vs. steric fields	9[c]	0.512 (2)[e]	0.931	0.022
8	log α vs. electrostatic and steric fields	18[d]	0.629 (4)	0.973	0.013

[a] CoMFA components used in the final models for Eqs. 6–8 are reported in parentheses.
[b] Referred to the X-substituted set I (compounds **1**–**10**).
[c] Referred to the R-substituted set II (compounds **4**, **12**–**19**).
[d] Whole set.
[e] Omitting compounds **16** and **17**, $q^2 = 0.817$.

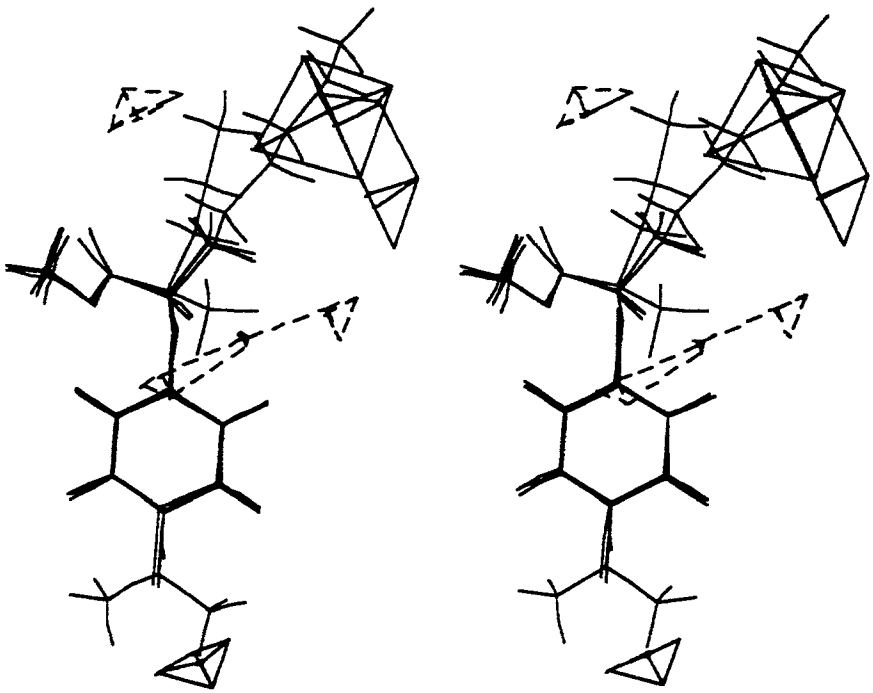

Fig. 2. Stereoview of the major steric features of CoMFA for the enantioseparation of esters **I**. The contour levels are –0.004 and 0.002 for dashed-line and solid-line polyhedra, respectively. The displayed molecules are **7**, **15** and **19**.

in the structural features of the different molecules in the data set lead to an increase or decrease in the target property (enantioseparation).

In Fig. 2 solid-line polyhedra define steric regions associated with an increase in log α (favourable interactions), whereas dashed-line polyhedra define regions associated with a decrease in enantioselective binding (unfavourable interactions). To aid visualization, compounds **7** (α = 1.69), **15** (α = 1.60) and **19** (α = 1.00) were overlayed with the steric contour map. A major favourable region around the α-alkyl moiety accounts for positive steric effects of R on the enhancement of α, whereas the 'repulsive' region close to the second alkyl group accounts for a detrimental effect of the alkyl groups (compounds **18** and **19** are not resolved). A favourable steric space close to X substituents indicates that substituents in the para position of the phenyl ring are well tolerated. Figure 3 shows the electrostatic CoMFA contour map for the enantioseparation of **I** on DACH-DNB (compounds **1**, **6**, **7** and **10**. Solid-line polyhedra contour the regions where decreasing negative charge enhances the enantioseparation, whereas dashed-line polyhedra contour the regions where log α increases if negative charge increases. The large dashed-line zone localized around the C(1') of the

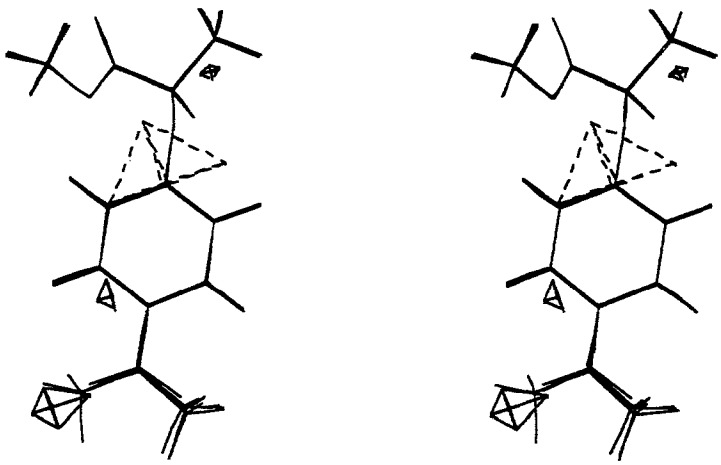

Fig. 3. Stereoview of the electrostatic CoMFA map for the enantioseparation of esters **I**. The contour levels are –0.005 and 0.009 for dashed-line and solid-line polyhedra, respectively. The displayed molecules are **1**, **6**, **7** and **10**.

phenyl ring indicates the importance of the π-electron-rich character of the aromatic moiety of the selected molecule in determining an enhancement of α. The decrease in the α value of congener **10** could be attributed to an unfavourable electrostatic interaction of the NO_2 substituent in the para position. Despite its quite good cross-validated r^2, the CoMFA model failed to predict the enantioseparation factor of compound **20** (α_{pred} = 1.31 vs. α_{obs} = 1.89 ($\log k'_S = 0.717$, $\log k'_R = 0.441$)). The enantioseparation factor of **20** was predicted to be very close to the value of its corresponding flexible analogue **4** (α = 1.29), despite the difference between their molecular structures. Compound **20** differs from **4** and all the other analogues examined in molecular rigidity. We believe that molecular rigidity, which is essentially an entropy-related factor, may account for the 'lower than predicted' α value of compound **20** [38,39]. On the other hand, as recognized by Cramer in the original paper on CoMFA [36], the CoMFA parameters (i.e., the molecular mechanics snapshot of steric and electrostatic nonbonded enthalpies) do not include entropically based factors, which should also contribute to the change in free energy related to the equilibrium of each enantiomer between the mobile and the stationary phase.

Conclusions

The investigation of the interaction mechanism of aryloxy acetic acid methyl esters **I** with the DACH-DNB CSP, by means of LFER and CoMFA approaches, has enabled us to formulate models that can rationalize the physicochemical factors affecting chiral recognition on a 'Pirkle-type' CSP.

LFER models derived in the present study revealed that solute lipophilicity and steric properties are the main factors responsible for retention of AAAE **I** on DACH-DNB CSP. The separation factor (α) varied mainly with electronic and steric properties of the examined solutes. The main difference between the mathematical model derived in the present study and that previously obtained for the enantioseparation of sulfoxides **II** is represented by the steric parameters, which correlate with log α linearly for AAAE **I** and parabolically for sulfoxides **II**. However, a closer examination of the two data sets reveals that this difference may be simply due to the different composition and (possibly) orientation of the R groups.

Compared to the classical LFER analysis, the 3D QSERR analysis allowed mixing of different sets of compounds for developing a quantitative 3D model of enantioselectivity. CoMFA, once again, demonstrated its usefulness in unraveling the complexity of steric and electrostatic interactions influencing enantioselective binding. While coefficient contour maps of the AAAE **I** solutes and the sulfoxides **II** are not exactly superposable, CoMFA has revealed a similar balance of physicochemical forces involved in the chiral recognition process on DACH-DNB. In a recent study similar forces were detected in the enantioseparation of benzimidazole sulfoxides on CHIRALPAK AD [40].

In summary, the present study presents further evidence on the potential of LFER and CoMFA approaches in understanding the mechanism of chiral recognition in chromatography and other related areas.

Acknowledgements

The authors express their thanks to Prof. Francesco Gasparrini, University 'La Sapienza', Rome, for the generous gift of the chiral stationary phase and to the C.N.R., Rome, Progetto Finalizzato Chimica Fine, for financial support. A.M.M. was supported by a Grant from the Bonino–Pulejo foundation, Messina, Italy.

References

1 Ariens, E.J., Wuis, E.W. and Veringa, E.J., Biochem. Pharmacol., 37 (1988) 9.
2 Caldwell, J., Winter, S.M. and Hutt, A.J., Xenobiotica, 18 (1988) 59.
3 De Camp, W.H., Chirality, 1 (1989) 2.
4 Cayen, M.N., Chirality, 3 (1991) 94.
5 Waldeck, B., Chirality, 5 (1993) 350.
6 Wainer, I.W. (Ed.) Drug Stereochemistry, Analytical Methods and Pharmacology, Marcel Dekker, New York, NY, 1993.
7 Nogradi, M., Stereoselective Synthesis, Weinheim, New York, NY, 1987.
8 Levin, S. and Abu-Lofi, S., Adv. Chromatogr., 33 (1993) 233.
9 Zief, M. and Crane, L.J. (Eds.) Chromatographic Chiral Separations, Marcel Dekker, New York, NY, 1988.
10 Stevenson, D. and Wilson, I.D. (Eds.) Chiral Separations, Plenum Press, New York, NY, 1989.
11 Allenmark, S.G. (Ed.) Chromatographic Enantioseparations: Methods and Applications, Ellis Horwood, Chichester, 1988.
12 Robert, S.M. (Ed.) Molecular Recognition: Chemical and Biochemical Problems, Royal Society of Chemistry, Cambridge, 1992.
13 Vögtle, F., Supramolecular Chemistry, Wiley, Chichester, 1991.
14 Altomare, C., Carotti, A., Cellamare, S., Fanelli, F., Gasparrini, C., Villani, C., Carrupt, P.-A. and Testa, B., Chirality, 5 (1993) 527.
15 Galli, B., Gasparrini, F., Misiti, D., Pierini, M. and Villani, C., Chromatographia, 24 (1987) 505.
16 Gasparrini, F., Misiti, D. and Villani, C., Chirality, 4 (1992) 447.
17 a. Bettoni, G., Loiodice, F., Tortorella, V., Conte-Camerino, D., Mambrini, M., Ferrannini, E. and Bryant, S.H., J. Med. Chem., 30 (1987) 1267.
b. Feller, D.L., Kamanna, V.S., Newman, H.A., Romstedt, K.J., Witiak, D.T., Bettoni, G., Loiodice, F., Conte-Camerino, D., Bryant, S.H. and Tortorella, V., J. Med. Chem., 30 (1987) 1265.
18 Ebenshade, T.A., Kamanna, V.S., Newman, H.A.I., Tortorella, V., Witiak, D.T. and Feller, D.R., Biochem. Pharmacol., 40 (1990) 1263.
19 De Luca, A.M., Tricarico, D., Wagner, R., Conte-Camerino, D., Tortorella, V. and Bryant, S.H., J. Pharmacol. Exp. Ther., 260 (1992) 364.
20 Bettoni, G., Ferorelli, S., Loiodice, F., Tangari, N., Tortorella, V., Gasparrini, F., Misiti, D. and Villani, C., Chirality, 4 (1992) 193.

21 Thibaut, U., Folkers, G., Klebe, G., Kubinyi, H., Merz, A. and Rognan, D., Quant. Struct.–Act. Relatsh., 13 (1994) 1.
22 Azzolina, O. and Ghislandi, V., Il Farmaco, 48 (1993) 713 and references cited therein.
23 Azzolina, O., Collina, S. and Ghislandi, V., Il Farmaco, 48 (1993) 1401.
24 Tambuté, A., Siret, L., Candé, M. and Rosset, S., J. Chromatogr., 541 (1991) 349.
25 Pirkle, W.H., Burke, J.A. and Wilson, S.R., J. Am. Chem. Soc., 111 (1989) 922.
26 Hansch, C. and Leo, A., Substituent Constants for Correlation Analysis in Chemistry and Biology, Wiley, New York, NY, 1979.
27 Dewar, M.J.S., Zoebisch, E.G., Healey, E.F. and Stewart, J.J.P., J. Am. Chem. Soc., 107 (1985) 3902.
28 Richards, W.G., Quantum Pharmacology, Butterworth, London, 1983.
29 Wilson, L.Y. and Famini, G.R., J. Med. Chem., 34 (1991) 1668.
30 Verloop, A., The STERIMOL Approach to Drug Design, Marcel Dekker, New York, NY, 1987.
31 Dearden, J.C., Brodburne, S.J.A. and Abraham, M.H., In Silipo, C. and Vittoria, A. (Eds.) QSAR: Rational Approaches to the Design of Bioactive Compounds, Elsevier, Amsterdam, 1991, pp. 143–150.
32 Leo, A., C-Log P Software, release 3.54, Daylight Chemical Information Systems Inc., Irvine, CA, 1991.
33 Van de Waterbeemd, H. and Testa, B., In Testa, B. (Ed.) Advances in Drug Research, Vol. 17, Academic Press, London, 1985, pp. 85–225.
34 Scott, P.P.W., In Simpon, C.F. (Ed.) Techniques in Ligand Chromatography, Wiley, New York, NY, 1992, pp. 141–184.
35 Dobashi, A., Dobashi, Y. and Hara, S., J. Liq. Chromatogr., 9 (1986) 243.
36 Cramer III, R.D., Patterson, D.E. and Bruce, J.D., J. Am. Chem. Soc., 110 (1988) 5959.
37 Cramer III, R.D., Bruce, J.D. and Patterson, D.E., Quant. Struct.–Act. Relatsh., 7 (1988) 18.
38 Klebe, G. and Abraham, U., J. Med. Chem., 36 (1993) 70.
39 DePriest, S.A., Mayer, D., Naylor, C.B. and Marshall, G.R., J. Am. Chem. Soc., 115 (1993) 5372.
40 Camilleri, P., Livingstone, D.J., Murphy, J.A. and Manallack, D.T., J. Comput.-Aided Mol. Design, 7 (1993) 291.